Intravitreal AAV2.COMP-Ang1 Attenuates Deep Capillary Plexus Expansion in the Aged Diabetic Mouse Retina

Lara S. Carroll,[1] Hironori Uehara,[1] Daniel Fang,[1] Susie Choi,[1] Xiaohui Zhang,[1] Malkit Singh,[1] Zoya Sandhu,[1] Philip M. Cummins,[2] Tim M. Curtis,[3] Alan W. Stitt,[3] Bonnie J. Archer,[1] and Balamurali K. Ambati[1]

[1]Moran Eye Center, Department of Ophthalmology and Visual Sciences, University of Utah, Salt Lake City, Utah, United States
[2]School of Biotechnology, Dublin City University, Glasnevin, Dublin, Ireland
[3]Wellcome-Wolfson Institute for Experimental Medicine, School of Medicine, Dentistry and Biomedical Sciences, Queen's University Belfast, Belfast, United Kingdom

Correspondence: Lara S. Carroll, Moran Eye Center, Department of Ophthalmology and Visual Sciences, University of Utah, 65 Mario Capecchi Drive, Salt Lake City, UT 84132, USA;
lsc3@utah.edu.

Submitted: November 8, 2018
Accepted: May 14, 2019

Citation: Carroll LS, Uehara H, Fang D, et al. Intravitreal AAV2.COMP-Ang1 attenuates deep capillary plexus expansion in the aged diabetic mouse retina. *Invest Ophthalmol Vis Sci*. 2019;60:2494–2502. https://doi.org/10.1167/iovs.18-26182

Purpose. We determine whether intravitreal angiopoietin-1 combined with the short coiled-coil domain of cartilage oligomeric matrix protein by adeno-associated viral serotype 2 (AAV2.COMP-Ang1) delivery following the onset of vascular damage could rescue or repair damaged vascular beds and attenuate neuronal atrophy and dysfunction in the retinas of aged diabetic mice.

Methods. AAV2.COMP-Ang1 was bilaterally injected into the vitreous of 6-month-old male $Ins2^{Akita}$ mice. Age-matched controls consisted of uninjected C57BL/6J and $Ins2^{Akita}$ males, and of $Ins2^{Akita}$ males injected with PBS or AAV2.REPORTER (AcGFP or LacZ). Retinal thickness and visual acuity were measured in vivo at baseline and at the 10.5-month endpoint. Ex vivo vascular parameters were measured from retinal flat mounts, and Western blot was used to detect protein expression.

Results. All three $Ins2^{Akita}$ control groups showed significantly increased deep vascular density at 10.5 months compared to uninjected C57BL/6J retinas (as measured by vessel area, length, lacunarity, and number of junctions). In contrast, deep microvascular density of $Ins2^{Akita}$ retinas treated with AAV2.COMP-Ang1 was more similar to uninjected C57BL/6J retinas for all parameters. However, no significant improvement in retinal thinning or diabetic retinopathy–associated visual loss was found in treated diabetic retinas.

Conclusions. Deep retinal microvasculature of diabetic $Ins2^{Akita}$ eyes shows late stage changes consistent with disorganized vascular proliferation. We show that intravitreally injected AAV2.COMP-Ang1 blocks this increase in deep microvascularity, even when administered subsequent to development of the first detectable vascular defects. However, improving vascular normalization did not attenuate neuroretinal degeneration or loss of visual acuity. Therefore, additional interventions are required to address neurodegenerative changes that are already underway.

Keywords: AAV2, diabetic retinopathy, intravitreal delivery, retina, vascular plexus

Diabetic retinopathy (DR) is the leading global cause of blindness in working individuals and one of the leading microvascular complications of diabetes.[1] Clinically, nonproliferative DR (NPDR) involves progressive damage of the retinal vessels with capillary dropout. Microvascular changes include microaneurysms, hemorrhages, and intraretinal microvascular abnormalities (IRMAs), which are tortuous intraretinal vascular segments. Progressive capillary dropout leads to hypoxia, proceeded by proliferating networks of leaky neovessels that can expand from the inner retina into the vitreous cavity – the hallmark of proliferative DR (PDR).

Diabetic hyperglycemia is toxic to the retinal microvasculature, disrupting endothelial tight junctions leading to breakdown of the blood-retinal barrier (BRB). Inflammatory mediators (i.e., TNF-α, IL-1β, and IL-6) upregulate adhesion molecules and growth factors (i.e., intercellular adhesion molecule–1 [ICAM-1] and VEGF), which in turn promote leukocyte-endothelial adhesion (54,55), a critical step in DR pathogenesis. Diabetes likely impairs the neural retina concurrent with (or before) vascular defects, as declines in visual electrophysiology can be detected in diabetic patients and animal models even before any clinically detectable symptoms of DR.[2,3] Chronic inflammation is likely a key factor in impairment of both the retinal microvasculature and the neural retina.[4–6]

Anti-VEGF therapies, such as ranibizumab and Aflibercept, arrest the pathologic angiogenesis of PDR, yet achieve temporary visual improvement in only a minority (23%–34%) of patients,[7–10] and therapies targeting alternative pathways to reverse progressive neurovascular dysfunction are needed. Type 1 Diabetic $Ins2^{Akita}$ mice suffer hyperglycemia by 4 weeks of age and show degenerative retinal changes by 6 months, including acellular capillaries, pericyte loss, retinal thinning, visual dysfunction, and b-wave diminution.[11–14] Although no rodent models faithfully recapitulate the vascular proliferation seen in human PDR, recent studies have reported an increase of

vascular density in the deep vascular plexus of aged diabetic db/db and $Ins2^{Akita}$ mice,[15–17] suggestive of the impaired vascular remodelling seen in "preproliferative" DR marked by IRMAs in human patients, a precursor of proliferative DR.[18,19]

Work in our and other laboratories suggests that Angiopoietin1 therapy can halt nonproliferative structural and functional changes associated with DR in mice, such as retinal thinning, acellular capillaries, and optokinetic tracking dysfunction.[13,20,21] The angiopoietins (Ang1 and Ang2) are secreted ligands that bind to the receptor tyrosine kinase Tie2 expressed on endothelial and hematopoietic cells. Whereas Ang2 is a context-dependent antagonist of Ang1/Tie2 signaling, Ang1 activation of Tie2 induces vessel survival, quiescence, and maturation, and decreases inflammation and leakiness in response to permeability-inducing inflammatory agents.[21,22] Our previous work has shown that sustained intravitreal expression of angiopoietin-1 combined with the short coiled-coil domain of cartilage oligomeric matrix protein (COMP-Ang1) by adeno-associated viral serotype 2 (AAV2.-COMP-Ang1) in 2-month old $Ins2^{Akita}$ males significantly attenuated capillary loss, breakdown of the BRB, and subsequent leukostasis, as well as preventing retinal thinning and loss of visual acuity, all of which occur in untreated $Ins2^{Akita}$ mice and DR patients.[11–14,16,23,24]

However, as progression of DR generally is well underway before clinical diagnosis, preventive management and early treatment is not an option for many patients. We show that delaying AAV2.COMP-Ang1 treatment well after DR onset was successful in preventing subsequent proliferative vascular retinopathy of the deep plexus in aged $Ins2^{Akita}$ mice. Despite this effect, delayed AAV2.COMP-Ang1 therapy did not attenuate progressive thinning of the peripheral retina, suggesting that additional nonvascular processes underlie susceptibility of neurons to chronic hyperglycemia, particularly once retinal thinning already is underway.

Methods

Animals

The type 1 diabetic $Ins2^{Akita}$ mouse on the C57BL/6J background was used to model DR. This animal harbors a mutation in the insulin gene that prevents proper insulin secretion. Heterozygous C57BL/6-$Ins2^{Akita}$/J ($Ins2^{Akita}$) males and healthy C57BL/6J female mice were obtained from the Jackson Laboratory (Sacramento, CA, USA) and crossed in our pathogen-free animal facility. As only male $Ins2^{Akita}$ mice consistently suffer diabetes, female pups were euthanized and male pups were genotyped at weaning (additional information in Supplementary Materials and Methods). Experiments were approved by the Institutional Animal Care and Use Committee of the University of Utah and conform to the ARVO Statement for the Use of Animals in Ophthalmic and Vision Research.

$Ins2^{Akita}$ mice were randomly assigned to an experimental treatment group: AAV2.COMP-Ang1 (carrying a 3′ FLAG tag for purification and immunodetection) or to one of three control groups: no injection, PBS, or AAV2.REPORTER (AcGFP or LacZ). All AAV2 constructs were driven by the CMV promoter. Wild type (WT) littermates received no ocular treatment (additional information provided in Supplementary Materials and Methods). High mortality of the aging $Ins2^{Akita}$ population precluded our ability to use equivalent numbers of each group for all assays. Six-month old $Ins2^{Akita}$ mice were treated with either 1 µL solution containing AAV2.COMP-Ang1, AAV2.REPORTER (2.0×10^9 viral genomes [VG]) or PBS injected into the vitreous cavity of both eyes.

In Vivo Imaging

In vivo retinal cross-sectional thickness was imaged bilaterally with optical coherence tomography (OCT; Spectralis HRA+OCT, Heidelberg Engineering, Heidelberg, Germany). Baseline thickness was measured in 6-month-old male $Ins2^{Akita}$ mice before intravitreal injections, in 10.5-month-old (±2 weeks) $Ins2^{Akita}$ and in age-matched WT littermates at both time points. OCT images were manually segmented and total retinal thickness was measured between the retinal nerve fiber layer (RNFL) and the basement membrane (BM) by an observer blinded to the treatment type. Four measurements corresponding to each of the retinal quadrants were averaged across both eyes at radial distances 0.5, 1.5, 2.5, 3.5, and 4.5 mm from the optic nerve head. Expression of the AAV2.AcGFP control vector in $Ins2^{Akita}$ mice was assessed in vivo using the FA imaging modality of the Heidelberg Spectralis (additional information provided in Supplementary Materials and Methods).

Immunofluorescent Labeling of Retinal Flat-Mounts

All procedures performed ex vivo were completed on retinas harvested at the experimental endpoint of 10.5 months (±2 weeks of age). See Supplementary Material and Methods for a detailed description of flat mount immunostaining and preparation.

Imaging and Image Processing

Vascular Quantification (Low Resolution), ×10 Objective. Equivalent fluorescence parameters were set using an EVOS FL imaging system to acquire ×10 stitched images of whole flat mounts labeled with fluorescent GS-IB4. Tiff images were inverted and transformed to grayscale in Photoshop (Adobe, San Jose, CA, USA) and imported into ImageJ (National Institutes of Health [NIH], Bethesda, MD, USA) for processing. In ImageJ, retinas were first outlined with the polygon tool, and the thresholding tool was used to convert all pixels to binary states by setting minimum and maximum thresholds = 230 (>230 = black, <230 = white). The total number of black and white pixels enclosed by the polygon was calculated and vessel density was calculated as #black/total pixels.

Deep Vascular Quantification (High Resolution), ×40 Objective. Efforts were taken to minimize sampling bias of the deep plexus as follows: Peripheral fields were manually selected using a Zeiss LSM 800 (×40 objective; Carl Zeiss Meditec, Jena, Germany) while focusing only within the superficial microvascular plane. After selecting each field, the focal plane was reset to the deep vascular plexus for imaging, and Z-stacks encompassing this layer were captured at 1 µm intervals. Supplementary Figure S1a shows that 1 µm interval distances are sufficient to image the deep vasculature while preventing confounding fluorescence from adjacent GS-IB4 fluorescent vascular beds.

Eight nonoverlapping fields within the retinal periphery (approximately 2.5 objective distances from the optic nerve) were selected across the four retinal quadrants. Images within each Z-stack were merged using ZEN lite (blue edition; Carl Zeiss Meditec) and the orthogonal projections were saved as tiff files for importing into Photoshop. A treatment-blind observer then manually masked extravascular cell types (infiltrating leukocytes, microglia, and macrophages) to eliminate this potential source of confounding GS-IB4 positive signal. Cleaned images subsequently were processed through AngioTool[25] (Supplementary Fig. S1B; available in the public domain at https://ccrod.cancer.gov/confluence/display/ROB2/Home), with equivalent parameter settings (intensity and

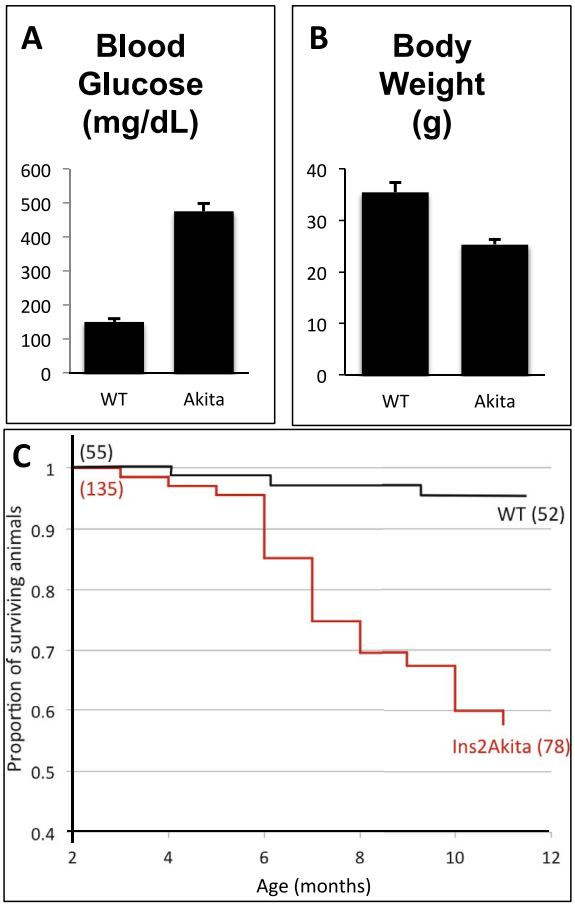

FIGURE 1. $Ins2^{Akita}$ mice show significant progression of diabetes by 6 months, including (**A**) elevated fasting blood glucose levels ($P < 0.0001$, Student's *t*-test) and (**B**) lower body weight ($P < 0.005$, Students *t*-test) relative to WT littermates. (**C**) $Ins2^{Akita}$ suffered significantly greater mortality than WT mice starting sharply at 6 months (logrank test, $P = 0.008$).

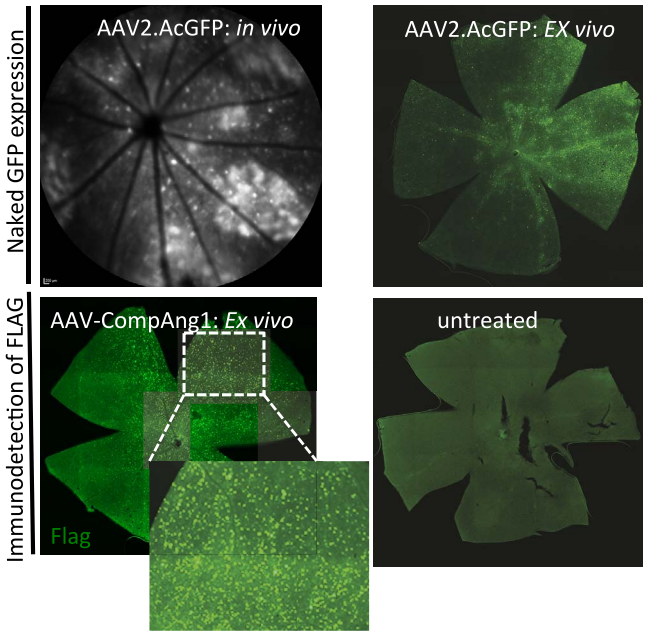

FIGURE 2. AAV2 expression is detectable 5 months after intravitreal injection. *Top*: The same retina was imaged for AAV2.AcGFP expression in vivo (*left*) by Spectralis FA mode, and ex vivo (*right*) by direct detection with GFP wavelength filter cube. *Bottom*: Indirect immunofluorescent detection of COMP-Ang1 using a FLAG tag in the AAV2.COMP-Ang1 viral construct (*left* + inset). FLAG signal is undetectable in untreated retinas (*right*).

vessel diameter range) across the entire dataset. The eight values representing eight separate peripheral retinal fields were averaged for each eye. Reported statistics are for: total vessels length, lacunarity,[26] (an index describing the distribution of the sizes of gaps, or "gappiness" within the image), number of vessel junctions, and vessels percentage area.

Optokinetic Tracking (OKT) for Visual Acuity

Optomotor reflex-based spatial frequency threshold tests were conducted on awake, unrestrained mice by a treatment-naïve operator using a visuomotor behavior measuring system (OptoMotry; CerebralMechanics, Lethbridge, AB, Canada). Presence or absence of the stimulus tracking response was established through repeated trials of varying direction and spatial frequency of the stimulus. Spatial frequency of the stimulus was stepped up or down with the staircase method to find the behavioral threshold, corresponding to the visual acuity for the behavior. Rotation speed (12°/s) and contrast (100%) were kept constant. WT and $Ins2^{Akita}$ mice underwent OKT at the 10.5-month endpoint.

Statistical Analysis

Numerical data were calculated in Excel (Microsoft, Redmond, WA, USA) and are presented as the mean ± SEM. The Student's 2-tailed *t*-test with a significance level of 0.05 was used to compare differences between two groups. For analysis of multiple groups, statistical analyses were performed with Past3 software.[27] Significant differences were first tested by ANOVA for $P < 0.05$, followed by Tukey's honest significant difference (HSD) test for pairwise comparisons of groups with unequal sample sizes.

Results

Mortality is Increased 7.8-Fold in Diabetic Mice

As expected, 6-month-old $Ins2^{Akita}$ males showed significantly elevated fasting blood glucose levels (Fig. 1A) and decreased body weights (Fig. 1B) relative to WT littermates (Glucose: WT, 149.8 ± 19.8 mg/dL; $Ins2^{Akita}$, 475.6 ± 52.4 mg/dL; Body Weight: WT, 35.4 ± 4.25 g; $Ins2^{Akita}$, 25.3 ± 2.1 g). Overall mortality rates increased sharply relative to WT littermates at approximately 6 months of age (Fig. 1C). Total mortality by the 10.5-month endpoint was 42.2% in $Ins2^{Akita}$ mice, but only 5.4% in WT mice, a 7.8-fold increase. Due to the increased fragility of aged $Ins2^{Akita}$ mice, we avoided procedures requiring extended use of anesthesia on these animals.

Diabetic Retinas Maintain Long-Term Viral Expression

Intraocular gene therapy was sustained for the duration of the experiments. Ex vivo images of AAV2.AcGFP injected retinal flat mounts show naked AcGFP expression consistent with in vivo imaging (Fig. 2). In vivo and ex vivo images showed fluorescent localization varying across retinal quadrants with the highest fluorescence close to the injection site. Expression of intravitreally injected AAV2.COMP-Ang1 was visualized in eight specimens by indirect immunofluorescent localization of

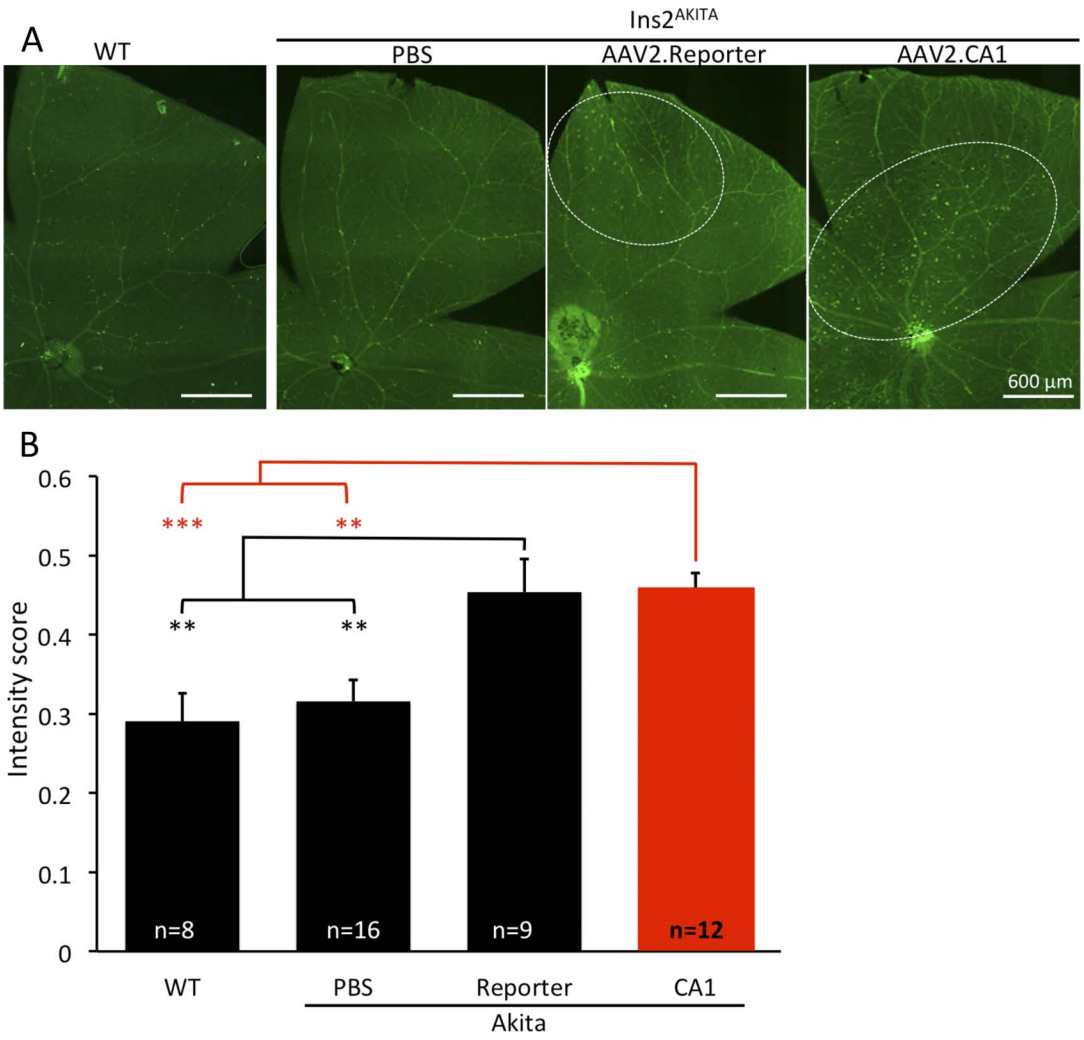

Figure 3. Isolectin B4 flat mounts of 10.5-month-old retinas. (**A**) GS-IB4-FITC lectin-labeled retinal flat mounts. Clusters of nonvascular cell types labeled by lectin are enclosed by ovals. (**B**) Retinas injected with AAV2 expression vectors had significantly higher intensity scores than WT or PBS-treated Ins2^{Akita} retinas. $^{**}P < 0.01$, $^{***}P < 0.001$.

the incorporated FLAG tag. No control retina exhibited FLAG-specific fluorescent signal (Fig. 2). Considerable variability in FLAG-immunofluorescent cell counts was found among AAV2.-COMP-Ang1–treated eyes, presumably due to variability in manual injections, and average number of COMP-Ang1–expressing cells varied over 5-fold among the eight FLAG-labeled retina. As COMP-Ang1 (and FLAG) is secreted extracellularly, this signal was lower than naked AcGFP signal in the AAV2.AcGFP injected retinas. Nevertheless, these data demonstrated that our AAV2 reagents can be targeted to (and sustained in) retinas following onset of DR for at least 5 months.

AAV2.COMP-Ang1 Prevents Proliferation of the Deep Vascular Network

We first attempted to assess vascularity at the experimental endpoint by measuring the total vascular signal in stitched ×10 objective images of GS-IB4-alexa488 labeled retinal flat mounts. Surprisingly, AAV2-treated diabetic retinas appeared more strongly labeled than those of WT and PBS-treated Ins2^{Akita} mice. Specifically, AAV2 expression vectors appeared to be associated with increased numbers of GS-IB4-alexa488 labeled monocytes/macrophages mostly confined to the superficial vascular plexus (Fig. 3A). Using the pan-macrophage/monocyte lineage marker Iba1, we found that approximately 85% of these extravascular cells labeled with GS-IB4 and Iba1 in Ins2^{Akita} retinas previously treated with intravitreal AAV2.LacZ or AAV2.COMP-Ang1 (Supplementary Fig. S2 and data not shown). Increased fluorescence of AAV2-treated diabetic retinas was confirmed by quantification of vascular signal across groups (Fig. 3B), indicating that the presence of GS-IB4–labeled extravascular cell types can introduce unacceptable bias to vascular quantification.

To obtain a more objective measure of retinal vascularity than the above low-resolution protocol, we imaged new cohorts of endpoint retinas that were labeled with GS-IB4-alexa647. Eight high-resolution ×40 confocal Z-stacks of the deep vascular plexus were captured approximately 2.5 objective diameters peripheral to the optic nerve and processed through AngioTool as per previous reports.[17,25,28] In contrast to the progressive capillary loss reported in studies (including ours) of younger Ins2^{Akita} mice,[13,29] retinas of the 10.5-month-old control Ins2^{Akita} mice demonstrated significant increases in total length and area of microvessels, number of

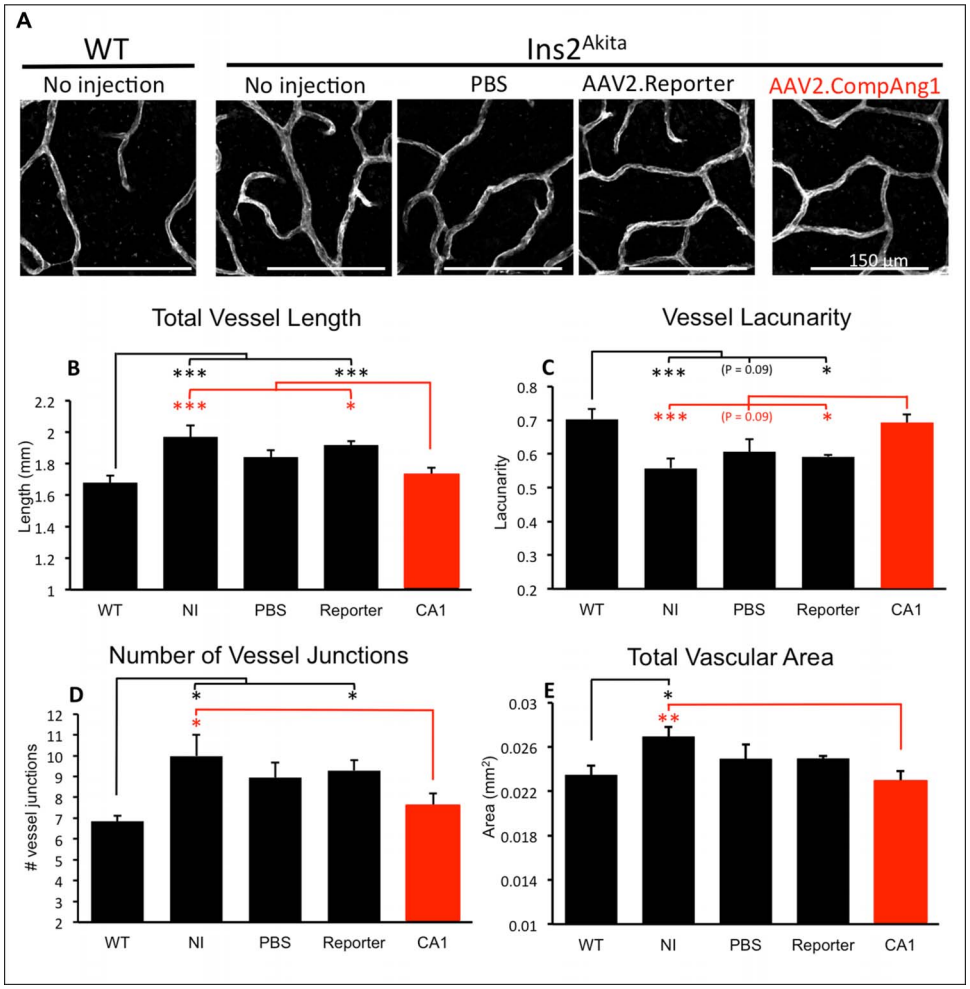

FIGURE 4. COMP-Ang1 treatment inhibits proliferative deep vascular remodeling in aged $Ins2^{Akita}$ retinas. (**A**) Representative ×40 confocal Z-stack images of WT and $Ins2^{Akita}$ deep plexus. (**B**–**E**) Several indices of vascularity: (**B**) vessel length, (**C**) lacunarity, (**D**) number of vessel junctions, and (**E**) vascular area indicate that between 6 and 10 months of age, the deep vascular plexus of $Ins2^{Akita}$ retinas is remodeled to increase vascular density relative to age-matched WT retinas (*black bars* and *asterisks*). In contrast, AAV2.COMP-Ang1–treated retinas were statistically more similar to WT retinas for all comparisons (*red bars* and *asterisks*). $N = 5$ (WT, NI, and PBS), $N = 8$ (Reporter), $N = 9$ (CA1) $^{*}P < 0.05$, $^{**}P < 0.01$, $^{***}P < 0.005$.

vessel junctions, and a decrease in lacunarity compared to untreated WT retinas (Fig. 4). Whereas all diabetic control groups showed an expansion of vessels in the deep vascular plexus, AAV2.Comp-Ang1–treated $Ins2^{Akita}$ retinas were comparable to WT retinas for all vascular measures, while differing significantly from $Ins2^{Akita}$ control groups, suggesting that Comp-Ang1 attenuated the diabetes-induced expansion of the deep vascular network.

Studies of diabetic rodents and humans show that ERK1/2 is activated in the diabetic retina, and may have a key role in glucose-mediated inflammatory induction.[30–33] Quantification of Western blot band intensities indicated that pERK1/2 protein levels of AAV2.COMP-Ang1–treated diabetic retinas were 41% lower than control diabetic retinas (Fig. 5A). However, this trend was not significant when comparing group means of WT, COMP-Ang1 $Ins2^{Akita}$, and control $Ins2^{Akita}$ retinas (ANOVA, $P = 0.23$). Interestingly, levels of membrane-bound (C-terminal) Tie2 were similar among all $Ins2^{Akita}$ control retinas, and insignificantly lower (20%) than Tie2 levels in WT retinas, suggesting that AAV2.COMP-Ang1–mediated vascular rescue was achieved without upregulating expression of its canonical receptor (Fig. 5B).

AAV2.COMP-Ang1 Treatment Does Not Prevent Retinal Thinning or Loss Of Visual Acuity in Six-Month-Old $Ins2^{Akita}$ Mice

Baseline and endpoint retinal thickness were measured and averaged across the four retinal quadrants at 1.5 mm incremental radial distances peripheral to the optic nerve head. Baseline retinal thickness of $Ins2^{Akita}$ retinas was significantly thinner than WT age-matched littermate retinas at all radial distances, and retinas of both genotypes continued to thin with age (Fig. 6A). However, AAV2-treated mice had expanded central retinas, tapering gradually toward the periphery, whereas thickness of WT and PBS-treated retinas was greatest at the 2.5 mm distance, tapering toward central retina and periphery (Figs. 6B–D). Despite the increased central retinal thickness, AAV2.COMP-Ang1 did not provide any protection from peripheral retinal thinning.

Peripheral retinal ganglion cell (RGC) counts (Supplementary Fig. S3) of WT, AAV2.COMP-Ang1– and PBS-injected eyes were significantly higher than peripheral RGC counts of AAV2.REPORTER–injected retinas (ANOVA, $P < 0.05$, Fig. 7A), suggesting potential neurotoxicity of chronic exogenous

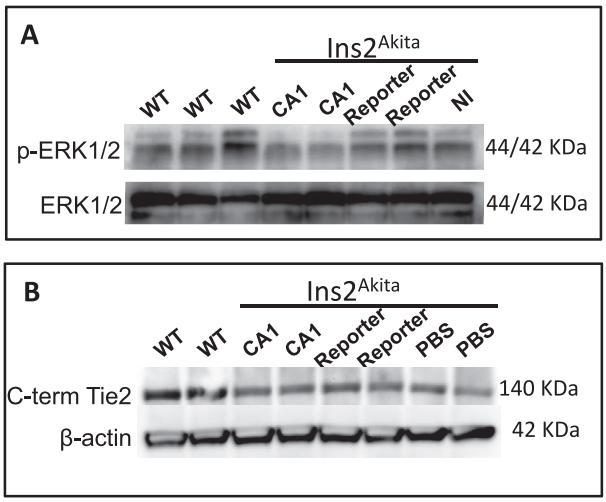

Figure 5. AAV2.COMP-Ang1 treatment reduced levels of phosphorylated ERK1/2 in the absence of Tie2 upregulation. (**A**) Protein levels of phosphorylated ERK1/2 in AAV2.COMP-Ang1 (CA1) retinas were 41% lower than diabetic control retinas, although this trend was not significant. (NI, no injection). (**B**) Retinal Tie2 receptor levels (C-terminal Tie2) of all Ins2^{Akita} groups were not significantly different from each other, but showed a trend of 20% less receptor protein than WT retinas.

reporter protein to this cell type in diabetic mice. Surprisingly, RGC counts of WT, PBS-injected, and AAV2.COMP-Ang1–injected retinas were not significantly different from each other, although we observed the trend: WT > AAV2.COMP-Ang1 > PBS.

Visual deficits arise early in DR patients and animal models, which can be measured as a decline in visual tracking behavior. We previously showed that Ins2^{Akita} mice treated with AAV2.COMP-Ang1 before DR symptoms were capable of resisting deterioration of optokinetic visual function.[13] However, consistent with the lack of rescue in retinal thickness, delaying AAV2.COMP-Ang1 treatment until 6 months failed to reverse or prevent further declines in visual acuity (Fig. 7B). Average right plus left eye acuity scores of all Ins2^{Akita} groups were significantly below those of WT mice ($P < 0.05$), but did not differ from each other.

Discussion

This study highlights important functional differences in Ang1/Tie2 signaling in the diabetic retina associated with disease progression and age. Studying proliferative DR remains a challenge. The rodent oxygen-induced retinopathy models exhibit rampant retinal neovascularization and are better correlates of retinopathy of prematurity, whereas the diabetic Akimba mouse has significant retinal cell loss. Neither the chronic models of Ins2^{Akita} nor db/db have the retinal

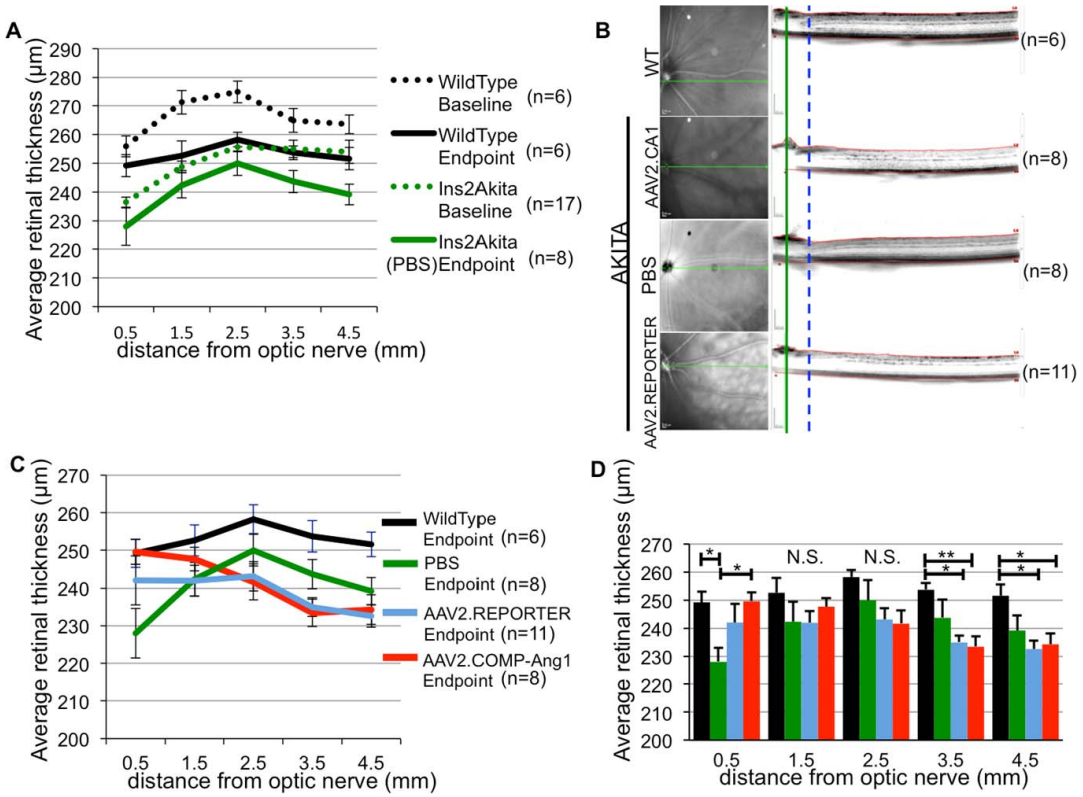

Figure 6. Retinal thinning was not prevented or improved after delayed COMP-Ang1 treatment. (**A**) Considerable retinal thinning occurred between baseline (6 months) and the experimental endpoint (10.5 months) in WT and Ins2^{Akita} mice. However, retinal thickness of Ins2^{Akita} mice was below that of age-matched WT littermates at all radial distances from the optic nerve head. (**B**) Representative images of HRA (*left*) and OCT images of all four study groups at the 10.5-month endpoint. The *dashed blue line* is at approximately 0.5 radial distance from the optic nerve head (*solid green line*). (**C**) Average retinal thickness at increasing radial distances from the optic nerve head is represented by a *colored line* for each group. Note that central retinas of the two AAV2-treated groups are considerably thicker than that of the PBS-injected group, whereas peripheral retinas of all Ins2^{Akita} groups are similar. (**D**) Same retinal thickness data (and color code) as in (**C**) but represented as bar graphs with pairwise comparisons performed at each radial distance that showed a significant difference among the group means. AAV2.COMP-Ang1 (AAV2.CA1) treatment did not prevent significant peripheral retinal thinning (*$P < 0.05$; **$P < 0.01$).

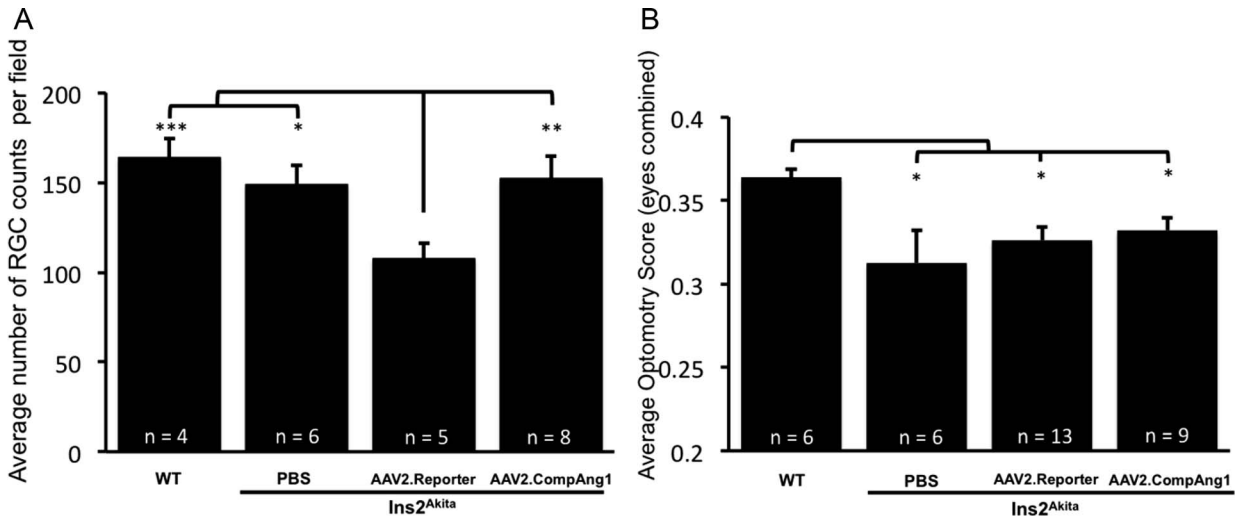

FIGURE 7. RGC and visual acuity loss. (**A**) RGC counts in retinal flat mounts immunolabeled with Brn3, compared across groups at the 10.5-month endpoint. RGC counts of AAV2.REPORTER treated $Ins2^{Akita}$ retinas were significantly lower than all other groups. (**B**) Averaged OD+OS OptoMotry scores of 10.5-month-old WT and Ins2Akita mice. All $Ins2^{Akita}$ mice showed significant loss of visual acuity compared to age-matched WT littermates at 10.5 months. $^{*}P < 0.05$, $^{**}P < 0.01$, and $^{***}P < 0.001$, respectively.

neovascularization seen in human patients. However, our confirmation that deep vascular proliferation occurs in diabetic mice provides the opportunity to explore therapies for normalizing proliferative remodeling in the adult diabetic retina.[15–17]

DR often is well advanced in patients before diagnosis. Therefore, it is critical to determine how therapeutic outcome varies with treatment initiated at later stages of disease. Novel treatments tested in rodent models are generally delivered before disease onset and studies terminate at or near 6 months of age before a sharp increase in diabetes-associated mortality occurs. Our study confirmed that beyond 6 months, the deep capillary plexus of $Ins2^{Akita}$ mice undergoes extensive proliferative remodeling at the retinal periphery. We suggested that this remodeling may reflect IRMAs found in human patients. IRMAs are proliferations that occur deeper in the retina than neovascularization and are likely a precursor to preretinal neovascularization.[18,19]

We demonstrated an antiangiogenic effect of AAV2.COMP-Ang1 in $Ins2^{Akita}$ retinas when delivery is initiated well after the establishment of diabetes, subsequent to pericyte dropout, capillary loss, and the onset of retinal thinning. Whereas early intervention with AAV2.COMP-Ang1 (at 2 months) halted the progression of vascular and neuronal impairment,[13] treatment at 6 months encountered an established inflammatory milieu with ongoing neurovascular degeneration. Yet even under these conditions, AAV2.COMP-Ang1 successfully mitigated persistent proangiogenic activity within the deep capillary bed, although it did not retard ongoing neuronal loss.

Body weights begin to diverge among diabetic and nondiabetic littermates soon after weaning and $Ins2^{Akita}$ males have significantly lower mass by 6 months. The fragility of aged diabetic males makes long-term studies challenging; we found a 7.8-fold increase in the mortality of our $Ins2^{Akita}$ mice relative to WT littermates, similar to a 5- to 10-fold increase in mortality risk for human patients with type1 diabetes.[34] As the general frailty of aged Ins2Akitas can contribute to behavioral changes among diabetic and nondiabetic littermates, this may exaggerate variation in behavioral tests of retinal function, such as OKT, which relies on the subtle head movements of subjects during visual tracking. Therefore, although we found no significant difference among OKT scores of control and treated $Ins2^{Akita}$ mice, it is important to note that diabetes-associated declines in behavioral responsiveness may confound the ability to detect improvements in visual acuity.

ERK1/2 phorphorylation is required for proproliferative, promigratory endothelial activity,[35] and is upregulated in the diabetic retinas of rodents and humans, drawing interest to its potential as a therapeutic target for DR.[20,31–33] Although Ang1/Tie2 signaling upregulates ERK1/2 phosphorylation in vitro,[36,37] Ang1 supplementation was reported previously to have the opposite effect in diabetic mouse retinas, reversing the diabetes-associated pERK1/2 increase.[20] Consistent with this, we found a strong trend (41%) of reduced pERK1/2 levels in diabetic retinas with AAV2.COMP-Ang1, even when treated after DR onset. However, the low number of retinal samples tested is a limitation of this analysis. Interestingly, levels of membrane-bound Tie2 receptor levels remained unchanged in AAV2.COMP-Ang1–treated diabetic retinas. As angiopoiteins can mediate endothelial activity via direct binding and induction of integrin pathways,[38,39] exploring the role of integrins in Ang1-mediated diabetic repair may be worthwhile.

AAV2.REPORTER and AAV2.COMP-Ang1 treatments led to infiltration of GS-IB4–labeled extravascular cells. We found that the panmacrophage/monocyte marker Iba1 colocalized with the majority of extravascular GS-IB4–labeled cells, suggesting an inflammatory identity. As AAV2 treatment also was associated with increased central retinal thickness suggestive of edema, we suspected that our AAV2 dosage (2×10^9 VG) is at the high end for retinas with established DR. Indeed, a previous report determined that diabetes enhances the retinal transduction and efficacy of AAV2 vectors,[40] suggesting that viral dose should be optimized at different time points following disease onset.

Using OCT angiography (OCTA), we recently confirmed that 6-month old $Ins2^{Akita}$ mice show significantly reduced perfusion, particularly in the deep vascular plexus.[29] Even temporary lack of motion contrast (blood flow) is undetectable by OCTA, and transient occlusive events are significantly more frequent in the deep capillary bed of $Ins2^{Akita}$ compared to WT mice.[41] Deep retinal ischemia resulting from diminished capillary perfusion at 6 months could explain why we found significant vascular expansion at the 10.5-month endpoint, since proliferative remodeling is the vascular response to

restore blood flow. Our future plans include longitudinal studies to further examine the association between hyperglycemia, retinal blood flow, and Tie2 modulation in the aging diabetic animal.

Acknowledgments

The authors thank Peter Barabas and Keith Rochfort for insightful discussion and feedback as well as two anonymous reviewers for their excellent suggestions to improve the manuscript.

Supported by National Eye Institute, NIH, Grants 5R01EY026029, Science Foundation Ireland US-Ireland R&D Partnership Programme (14/US/B3116; PMC), Northern Ireland Health and Social Care R&D Division (STL/4748/13; TMC, AWS), and the Medical Research Council (MC_PC_15026; TMC, AWS), and in part by an unrestricted grant from Research to Prevent Blindness, Inc., New York, NY, to the Department of Ophthalmology and Visual Sciences, University of Utah.

Disclosure: **L.S. Carroll**, None; **H. Uehara**, None; **D. Fang**, None; **S. Choi**, None; **X. Zhang**, None; **M. Singh**, None; **Z. Sandhu**, None; **P.M. Cummins**, None; **T.M. Curtis**, None; **A.W. Stitt**, None; **B.J. Archer**, None; **B.K. Ambati**, None

References

1. Bourne RR, Stevens GA, White RA, et al. Causes of vision loss worldwide, 1990-2010: a systematic analysis. *Lancet Glob Health*. 2013;1:e339–e349.
2. Lynch SK, Abramoff MD. Diabetic retinopathy is a neurodegenerative disorder. *Vis Res*. 2017;139:101–107.
3. Sohn EH, van Dijk HW, Jiao C, et al. Retinal neurodegeneration may precede microvascular changes characteristic of diabetic retinopathy in diabetes mellitus. *Proc Natl Acad Sci U S A*. 2016;113:E2655–E2664.
4. Joussen AM, Poulaki V, Le ML, et al. A central role for inflammation in the pathogenesis of diabetic retinopathy. *FASEB J*. 2004;18:1450–1452.
5. Rubsam A, Parikh S, Fort PE. Role of inflammation in diabetic retinopathy. *Int J Mol Sci*. 2018;19:E942.
6. Yu Y, Chen H, Su SB. Neuroinflammatory responses in diabetic retinopathy. *J Neuroinflam*. 2015;12:141.
7. Mitchell P, Bandello F, Schmidt-Erfurth U, et al. The RESTORE study: ranibizumab monotherapy or combined with laser versus laser monotherapy for diabetic macular edema. *Ophthalmology*. 2011;118:615–625.
8. Nguyen QD, Shah SM, Heier JS, et al. Primary end point (six months) results of the ranibizumab for edema of the mAcula in diabetes (READ-2) study. *Ophthalmology*. 2009;116:2175–2181.
9. Nguyen QD, Shah SM, Khwaja AA, et al. Two-year outcomes of the ranibizumab for edema of the mAcula in diabetes (READ-2) study. *Ophthalmology*. 2010;117:2146–2151.
10. Heier JS, Boyer D, Nguyen QD, et al. The 1-year results of CLEAR-IT 2, a phase 2 study of vascular endothelial growth factor trap-eye dosed as-needed after 12-week fixed dosing. *Ophthalmology*. 2011;118:1098–1106.
11. Francis AW, Wanek J, Shahidi M. Assessment of global and local alterations in retinal layer thickness in Ins2 (Akita) diabetic mice by spectral domain optical coherence tomography. *J Ophthalmol*. 2018;2018:7253498.
12. Barber AJ, Antonetti DA, Kern TS, et al. The Ins2Akita mouse as a model of early retinal complications in diabetes. *Invest Ophthalmol Vis Sci*. 2005;46:2210–2218.
13. Cahoon JM, Rai RR, Carroll LS, et al. Intravitreal AAV2.COMP-Ang1 Prevents Neurovascular degeneration in a murine model of diabetic retinopathy. *Diabetes*. 2015;64:4247–4259.
14. Hombrebueno JR, Chen M, Penalva RG, Xu H. Loss of synaptic connectivity, particularly in second order neurons is a key feature of diabetic retinal neuropathy in the Ins2Akita mouse. *PLoS One*. 2014;9:e97970.
15. Cheung AK, Fung MK, Lo AC, et al. Aldose reductase deficiency prevents diabetes-induced blood-retinal barrier breakdown, apoptosis, and glial reactivation in the retina of db/db mice. *Diabetes*. 2005;54:3119–3125.
16. Han Z, Guo J, Conley SM, Naash MI. Retinal angiogenesis in the Ins2(Akita) mouse model of diabetic retinopathy. *Invest Ophthalmol Vis Sci*. 2013;54:574–584.
17. McLenachan S, Magno AL, Ramos D, et al. Angiography reveals novel features of the retinal vasculature in healthy and diabetic mice. *Exp Eye Res*. 2015;138:6–21.
18. Fundus photographic risk factors for progression of diabetic retinopathy. ETDRS report number 12. Early Treatment Diabetic Retinopathy Study Research Group. *Ophthalmology*. 1991;98:823–833.
19. Lee CS, Lee AY, Baughman D, et al. The United Kingdom Diabetic Retinopathy Electronic Medical Record Users Group: report 3: baseline retinopathy and clinical features predict progression of diabetic retinopathy. *Am J Ophthalmol*. 2017;180:64–71.
20. Joussen AM, Poulaki V, Tsujikawa A, et al. Suppression of diabetic retinopathy with angiopoietin-1. *Am J Pathol*. 2002;160:1683–1693.
21. Thurston G, Suri C, Smith K, et al. Leakage-resistant blood vessels in mice transgenically overexpressing angiopoietin-1. *Science*. 1999;286:2511–2514.
22. Augustin HG, Koh GY, Thurston G, Alitalo K. Control of vascular morphogenesis and homeostasis through the angiopoietin-Tie system. *Nat Rev Mol Cell Biol*. 2009;10:165–177.
23. Barber AJ, Lieth E, Khin SA, et al. Neural apoptosis in the retina during experimental and human diabetes. Early onset and effect of insulin. *J Clin Invest*. 1998;102:783–791.
24. Muir ER, Renteria RC, Duong TQ. Reduced ocular blood flow as an early indicator of diabetic retinopathy in a mouse model of diabetes. *Invest Ophthalmol Vis Sci*. 2012;53:6488–6494.
25. Zudaire E, Gambardella L, Kurcz C, Vermeren S. A computational tool for quantitative analysis of vascular networks. *PLoS One*. 2011;6:e27385.
26. Gould DJ, Vadakkan TJ, Poche RA, Dickinson ME. Multifractal and lacunarity analysis of microvascular morphology and remodeling. *Microcirculation*. 2011;18:136–151.
27. Hammer O, Harper DA, Ryan P. Past: paleontological statistics software package for education and data analysis. *Palaeontol Electron*. 2001;4:1–9.
28. Giannakaki-Zimmermann H, Kokona D, Wolf S, Ebneter A, Zinkernagel MS. Optical coherence tomography angiography in mice: comparison with confocal scanning laser microscopy and fluorescein angiography. *Trans Vis Sci Tech*. 2016;5(4):11.
29. Uehara H, Lesuma T, Stocking P, et al. Detection of microvascular retinal changes in type I diabetic mice with optical coherence tomography angiography. *Exp Eye Res*. 2019;178:91–98.
30. Abu-El-Asrar AM, Dralands L, Missotten L, Al-Jadaan IA, Geboes K. Expression of apoptosis markers in the retinas of human subjects with diabetes. *Invest Ophthalmol Vis Sci*. 2004;45:2760–2766.
31. Mohammad G, Mairaj Siddiquei M, Imtiaz Nawaz M, Abu El-Asrar AM. The ERK1/2 inhibitor U0126 attenuates diabetes-induced upregulation of MMP-9 and biomarkers of inflammation in the retina. *J Diabetes Res*. 2013;2013:658548.
32. Ye X, Xu G, Chang Q, et al. ERK1/2 signaling pathways involved in VEGF release in diabetic rat retina. *Invest Ophthalmol Vis Sci*. 2010;51:5226–5233.
33. Mohammad G, Kowluru RA. Diabetic retinopathy and signaling mechanism for activation of matrix metalloproteinase-9. *J Cell Physiol*. 2012;227:1052–1061.

34. Miller RG, Mahajan HD, Costacou T, et al. A contemporary estimate of total mortality and cardiovascular disease risk in young adults with type 1 diabetes: the Pittsburgh Epidemiology of Diabetes Complications Study. *Diabetes Care*. 2016;39:2296–2303.
35. Srinivasan R, Zabuawala T, Huang H, et al. Erk1 and Erk2 regulate endothelial cell proliferation and migration during mouse embryonic angiogenesis. *PLoS One*. 2009;4:e8283.
36. Fukuhara S, Sako K, Noda K, et al. Tie2 is tied at the cell-cell contacts and to extracellular matrix by angiopoietin-1. *Exp Mol Med*. 2009;41:133–139.
37. Fukuhara S, Sako K, Noda K, et al. Angiopoietin-1/Tie2 receptor signaling in vascular quiescence and angiogenesis. *Histol Histopathol*. 2010;25:387–396.
38. Carlson TR, Feng Y, Maisonpierre PC, Mrksich M, Morla AO. Direct cell adhesion to the angiopoietins mediated by integrins. *J Biol Chem*. 2001;276:26516–26525.
39. Dalton AC, Shlamkovitch T, Papo N, Barton WA. Constitutive association of Tie1 and Tie2 with endothelial integrins is functionally modulated by angiopoietin-1 and fibronectin. *PLoS One*. 2016;11:e0163732.
40. Diaz-Lezama N, Wu Z, Adan-Castro E, et al. Diabetes enhances the efficacy of AAV2 vectors in the retina: therapeutic effect of AAV2 encoding vasoinhibin and soluble VEGF receptor 1. *Lab Invest*. 2016;96:283–295.
41. Wright WS, Yadav AS, McElhatten RM, Harris NR. Retinal blood flow abnormalities following six months of hyperglycemia in the Ins2(Akita) mouse. *Exp Eye Res*. 2012;98:9–15.

Investigative Ophthalmology & Visual Science